Supplementary Figures and Tables

Journal: Nature Medicine

Article Title	ROR-γ drives androgen receptor expression and represents a therapeutic target in castration-resistant prostate cancer
Corresponding Author:	Hong-Wu Chen and Yong Xu

Supplementary Item	**Title**
Supplementary Figure 1	Overexpression of ROR-γ, not ROR-α or ROR-β, associates with metastatic CRPC progression.
Supplementary Figure 2	Design strategy of ROR-γ antagonist XY018.
Supplementary Figure 3	ROR-γ antagonists potently inhibit growth and survival of CRPC cells.
Supplementary Figure 4	ROR-γ antagonists strongly inhibit AR signaling.
Supplementary Figure 5	Control of AR and its variant expression by ROR-γ in prostate cancer cells and the likelihood in clinical tumors.
Supplementary Figure 6	The effects of ROR-γ inhibition on AR genome binding, histone modifications, and Pol-II recruitment.
Supplementary Figure 7	ROR-γ antagonists inhibit AR function through suppression of AR expression.
Supplementary Figure 8	ROR-γ directly controls *AR* gene expression through binding an exonic RORE and recruiting SRCs.
Supplementary Figure 9	*In Vivo* effects of ROR-γ antagonists or shRNA on growth of prostate cancer xenograft tumors and mouse body weight
Supplementary Figure 10	ROR-γ inhibition strongly suppresses AR and its variant expression and eliminates AR binding *in vivo*.
Supplementary Figure 11	*In vivo* effects of ROR-γ antagonists on normal mouse prostate and testis.
Supplementary Figure 12	Lack of inhibitory effects by ROR-γ antagonists on AR expression in non-malignant, human prostate epithelial cells.
Supplementary Table 1	Antibodies for immunoblotting
Supplementary Table 2	Primers for qPCR and ChIP assay
Supplementary Table 3	siRNA sequence

Supplementary Figure 1

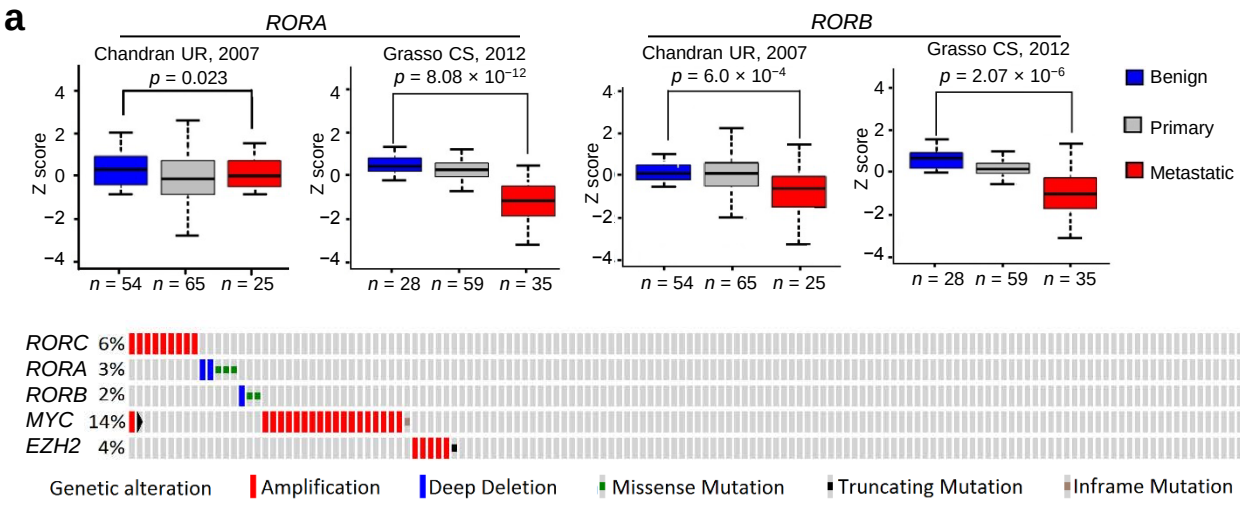

b

		Score 0-1 N	Score 2-3 N	*P* Value
All stages		34	36	
Stage	I-II	25	9	
	III-IV	9	27	=4.9E-05
Gleason score				
	≤7	15	1	
	8-10	22	27	=0.0006
Metastasis (Met)				
	Primary	23	22	
	Met	3	22	=0.0012

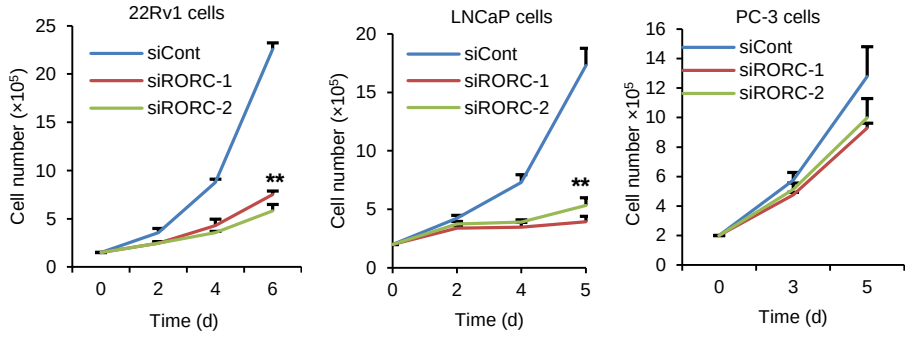

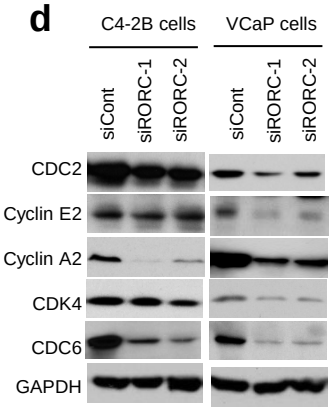

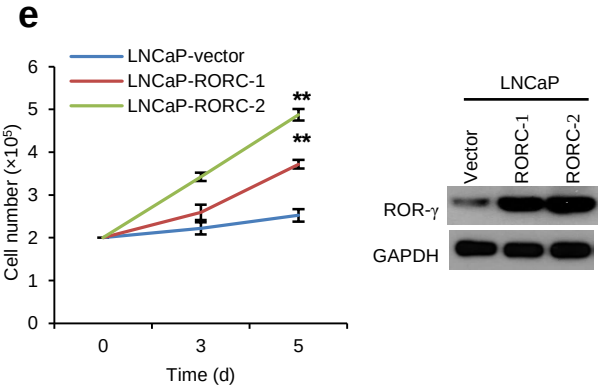

Supplementary Figure 1. Overexpression of ROR-γ, not ROR-α or ROR-β, associates with metastatic CRPC progression

(a) *RORA* and *RORB* transcript expression in two prostate cancer microarray studies from the GEO database. Data sets were analyzed for the transcript levels of *RORA* and *RORB* genes, which encode ROR-α and ROR-β proteins respectively, in benign prostate tissues, and primary or metastatic prostate tumor tissues (top). Oncoprint display from cBioPortal (http://www.cbioportal.org) of the three *ROR* gene alterations in metastatic prostate cancer tumors from 150 patients reported in a recent study[45] (bottom). *MYC* and *EZH2* are displayed for comparison of their alteration frequency and individual tumor relationship with the three *ROR* genes in the same study.

(b) Immunohistochemistry (IHC) analysis of association of ROR-γ protein levels with pathological parameters in a cohort of prostate cancer tumor specimens (n = 70).

(c) VCaP, 22Rv1, LNCaP and PC-3 cells were transfected with RORC or control siRNA. After indicated time, cells were harvested for determining cell growth by counting viable cells. n = 3.

(d) C4-2B and VCaP cells were transfected with RORC or control siRNA. Three days later, cells were harvested for immunoblotting with indicated antibodies.

(e) LNCaP cells were infected by ROR-γ overexpressing or control lentiviruses and stable pools of infected cells were cultured in charcoal-dextran-stripped (cds) FBS supplemented medium. After indicated times, cells were harvested for determining cell growth by counting viable cells, n = 3. Cells in regular medium were harvested for immunoblotting with ROR-γ or GAPDH antibodies.

Data are shown as mean ± s.d. Significance was calculated using Student's t-test. ** $p < 0.001$.

Supplementary Figure 2

a

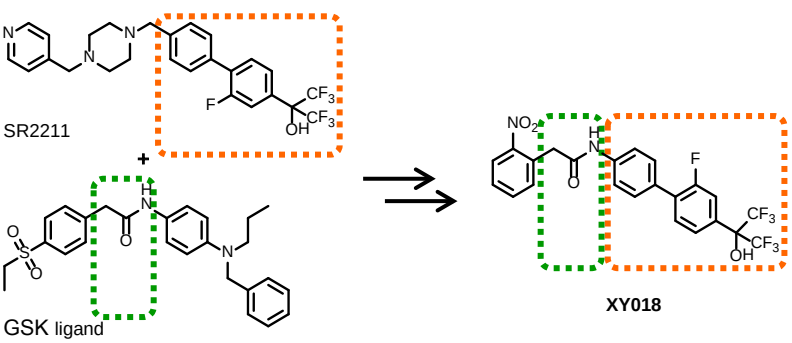

b

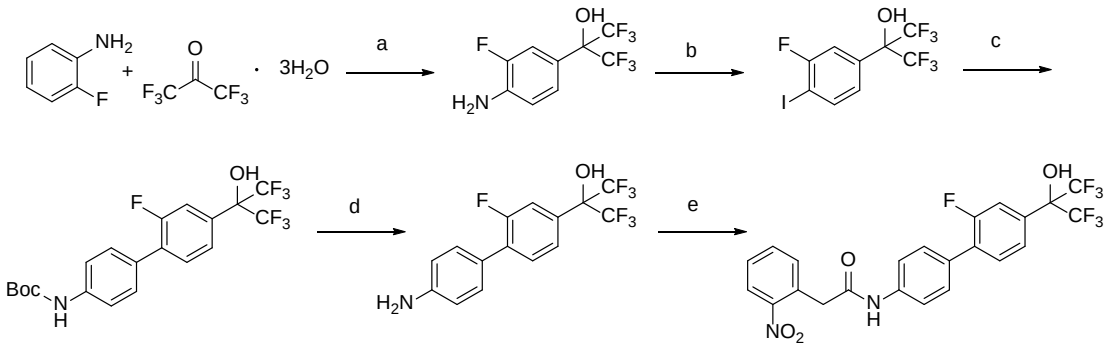

c

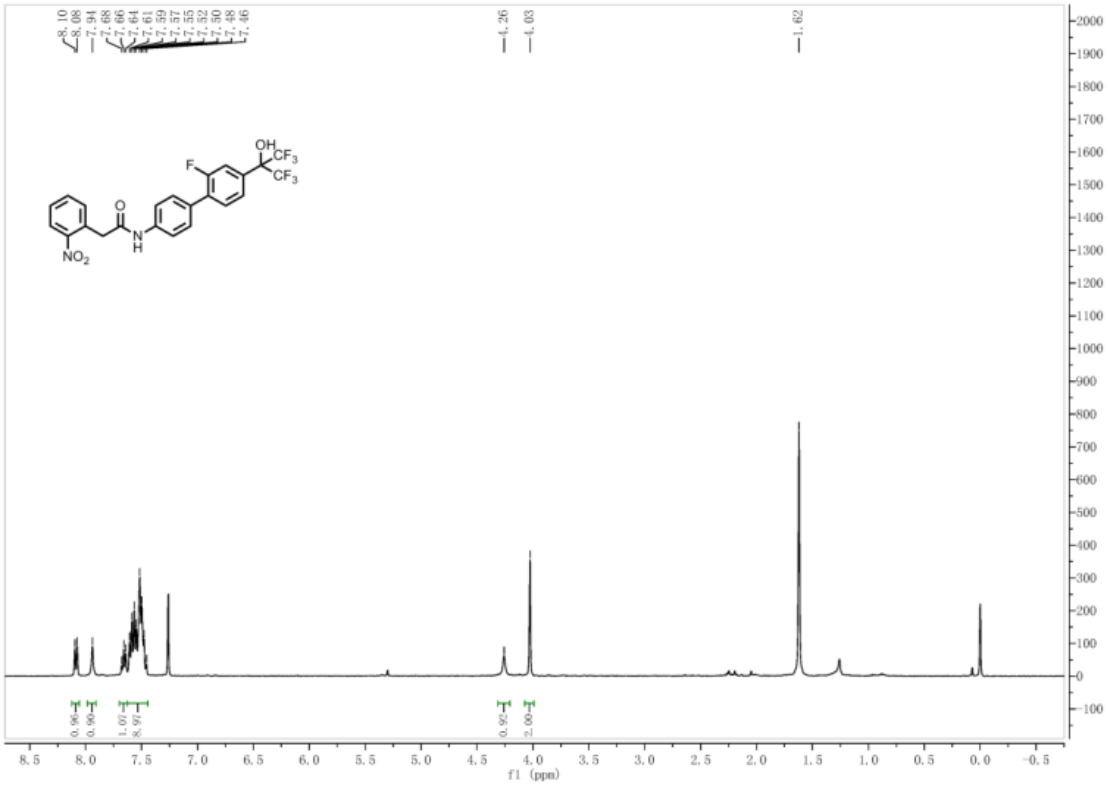

d

RORγ activity (μM)

	SR2211	XY018
EC_{50} on ROR-γ Activity	0.085 ± 0.01	0.19±0.02
Alpha Screen	0.93±0.05	3.46±1.32
TSA (ΔT)	6.5 ℃	4.2 ℃

e

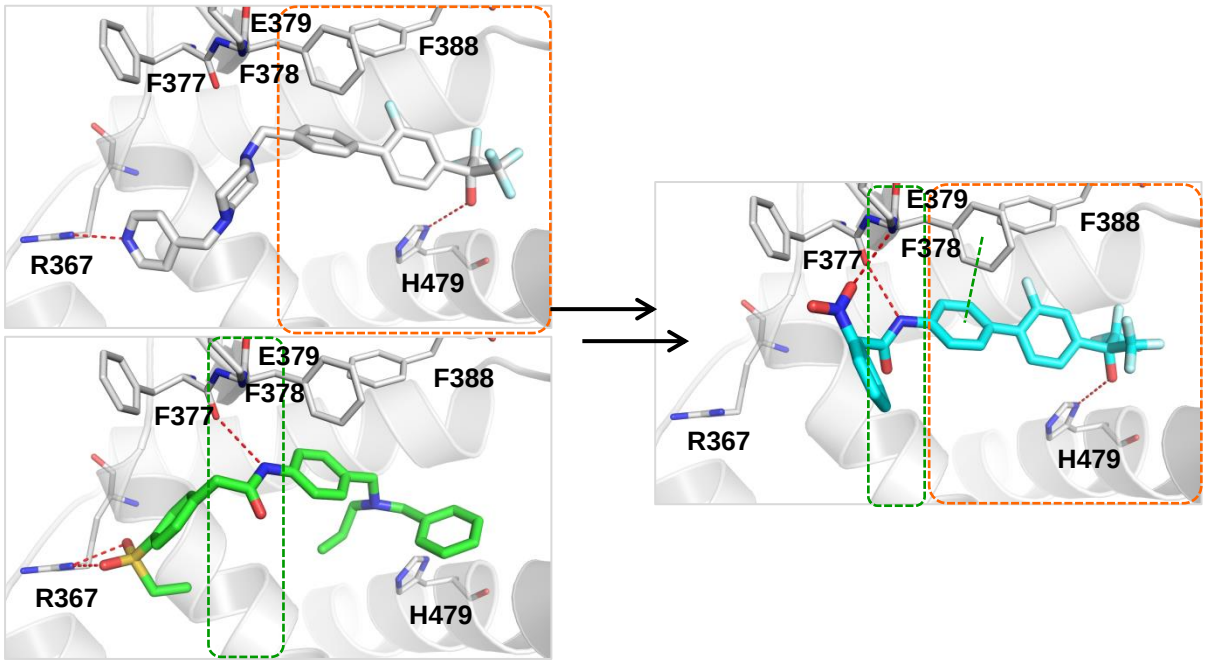

f

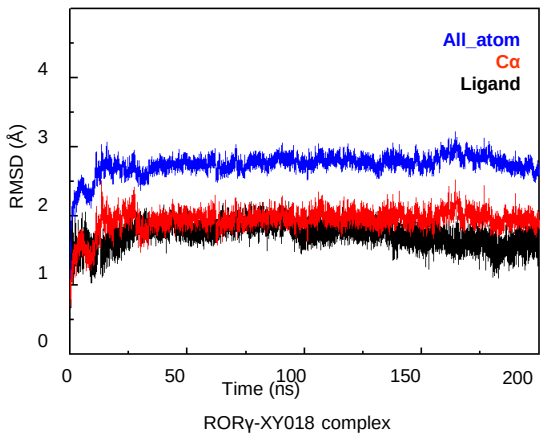

RORγ-XY018 complex

Supplementary Figure 2. Design and synthesis of ROR-γ antagonist XY018

(a) ROR-γ antagonist XY018 was designed based on SR2211 and the GSK ligand. The 2-([1,1'-biphenyl]-4-yl)-1,1,1,3,3,3-hexafluoropropan-2-ol group of SR2211 was kept, while amide group of the GSK agonist was chosen as linker.

(b) Synthesis scheme of compound XY018. Reagents and conditions: (a) p-toluenelsuphonic acid, 90℃, 30%; (b) HCl, NaNO2, DMF, 0-5℃; KI, 0℃-rt, 96%; (c) (4-((tert-butoxycarbonyl)amino)phenyl)boronic acid, Pd(PPh3)4, K2CO3, 1,4-dioxane, 80℃, 74 %; (d) TFA, DCM, rt, 91%; (e) 2-(2-nitrophenyl)acetic acid, HATU, DIPEA, DCM, rt, 81%.

(c) ^{1}H NMR spectrum of XY018.

(d) ROR-γ transcriptional activity was measured by reporter gene assay in 293T cells with Gal4-ROR-γ LBD expression vectors. EC_{50} values are reported as means ± s.d. for ≥ 8 separate titrations from 10 μM. *In vitro* binding to the LBD was measured by AlphaScreen and by TSA.

(e) Designed molecules were docked into the ROR-γ LBD by using Glide docking program with SP score. XY018 was obtained after extensive optimization of the left-side portion. The predicted preferable binding mode was shown. Hydrogen bond interactions are shown as dash lines in red while π-π interaction is shown as dash line in green. For clarity, only the key residues in the pocket are shown.

(f) Molecular dynamics demonstrated that the XY018 and ROR-γ complex is very stable with its predicted conformation. RMSD for ligand (black), Cα (red) and all atoms (blue) are shown for 200 ns simulation.

Supplementary Figure 3

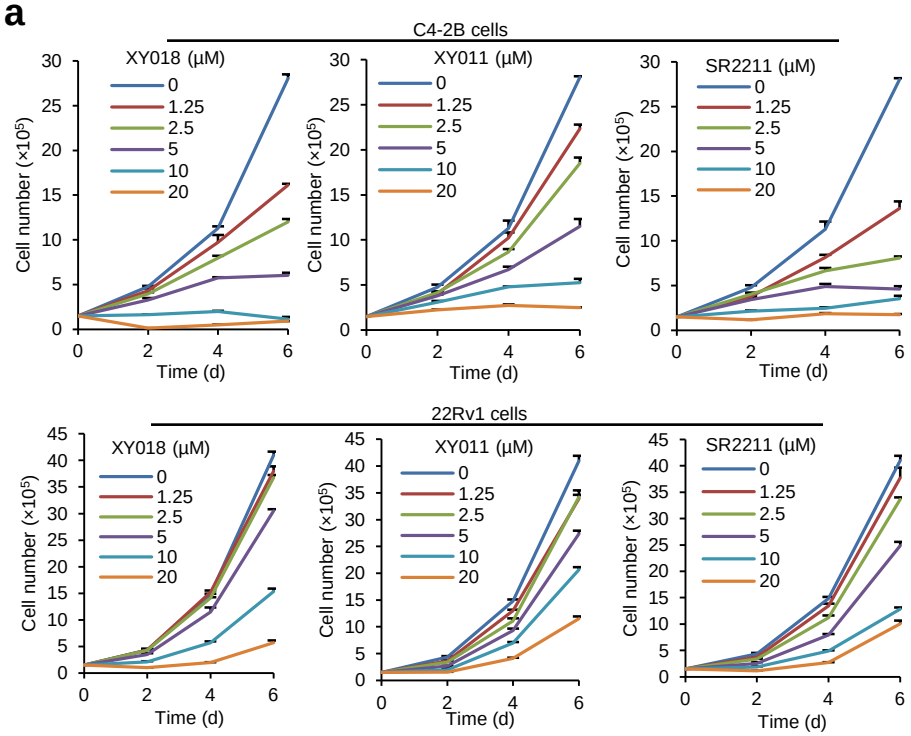

b

Cell line	AR status	IC_{50} (μM) SR2211	IC_{50} (μM) ENZ
LNCaP	Positive	1.5	32.5
C4-2B	Positive	2.1	45.5
LAPC4	Positive	3.2	43.3
VCaP	Positive	3.7	29.5
PC346C	Positive	4.8	35.7
22RV1	Positive	5.4	>50
PC-3	Negative	36.2	>50
PNT2	Negative	51.5	
RWPE1	Low	48.9	
IMR90	Negative	40.0	

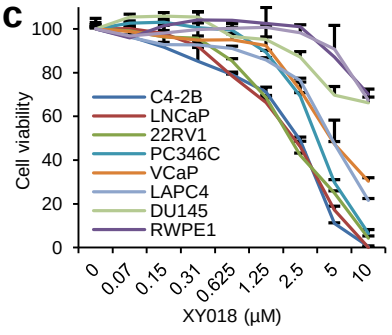

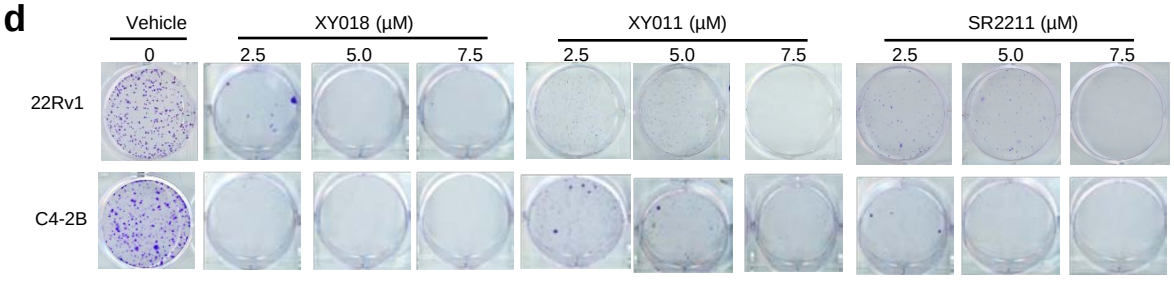

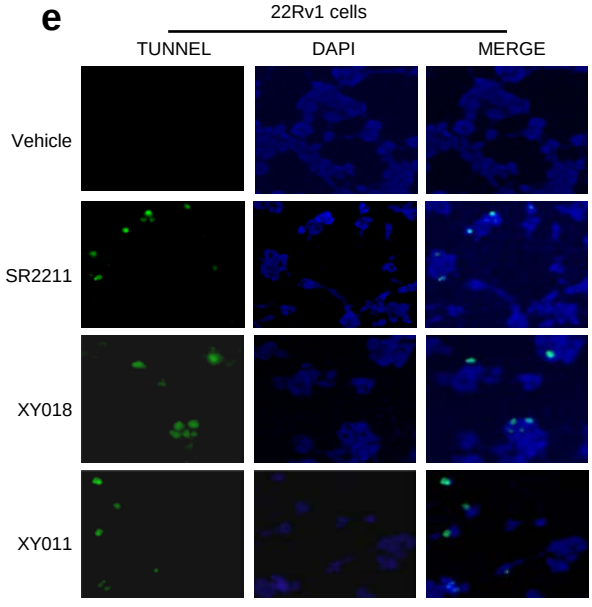

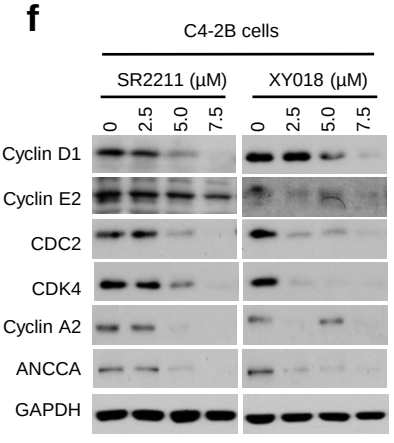

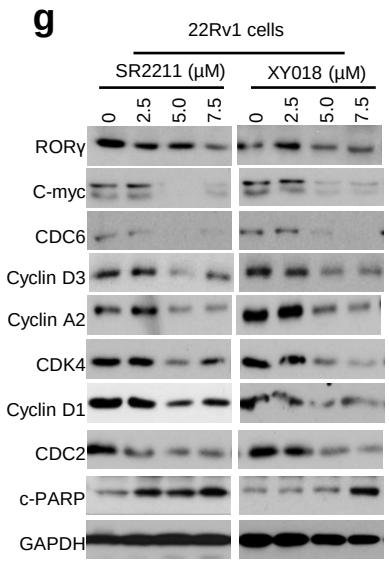

Supplementary Figure 3. ROR-γ antagonists potently inhibit growth and survival of CRPC cells

(a) C4-2B and 22Rv1cell proliferation after the ROR-γ antagonist treatment. Cells were seeded in 6-well plates and counted after cells were treated with indicated concentrations of ROR-γ antagonists for 0, 2, 4 and 6 days by Coulter counter. Data are showed as mean ± s.d. $n = 3$.

(b) Half-maximum inhibitory concentration (IC_{50}) for SR2211 and ENZ in indicated cell lines treated for 4 days is shown.

(c) Cell viability curves measured by CellTiter-GLO for different cells treated with ROR-γ antagonist XY018 or vehicle for 4 days. Data are showed as mean ± s.d. $n = 3$.

(d) Representative images of colony formation of C4-2B and 22Rv1 cells treated with vehicle, SR2211, XY018 or XY011 for 14 days,

(e) Representative images of TUNEL positive cells treated with vehicle or the antagonists (5 μM) in 22Rv1 cells are shown.

(f) and (g) C4-2B and 22Rv1 cells were treated with vehicle, XY018 or SR2211. Three days later, cells were harvested for immunoblotting with indicated antibodies.

Supplementary Figure 4

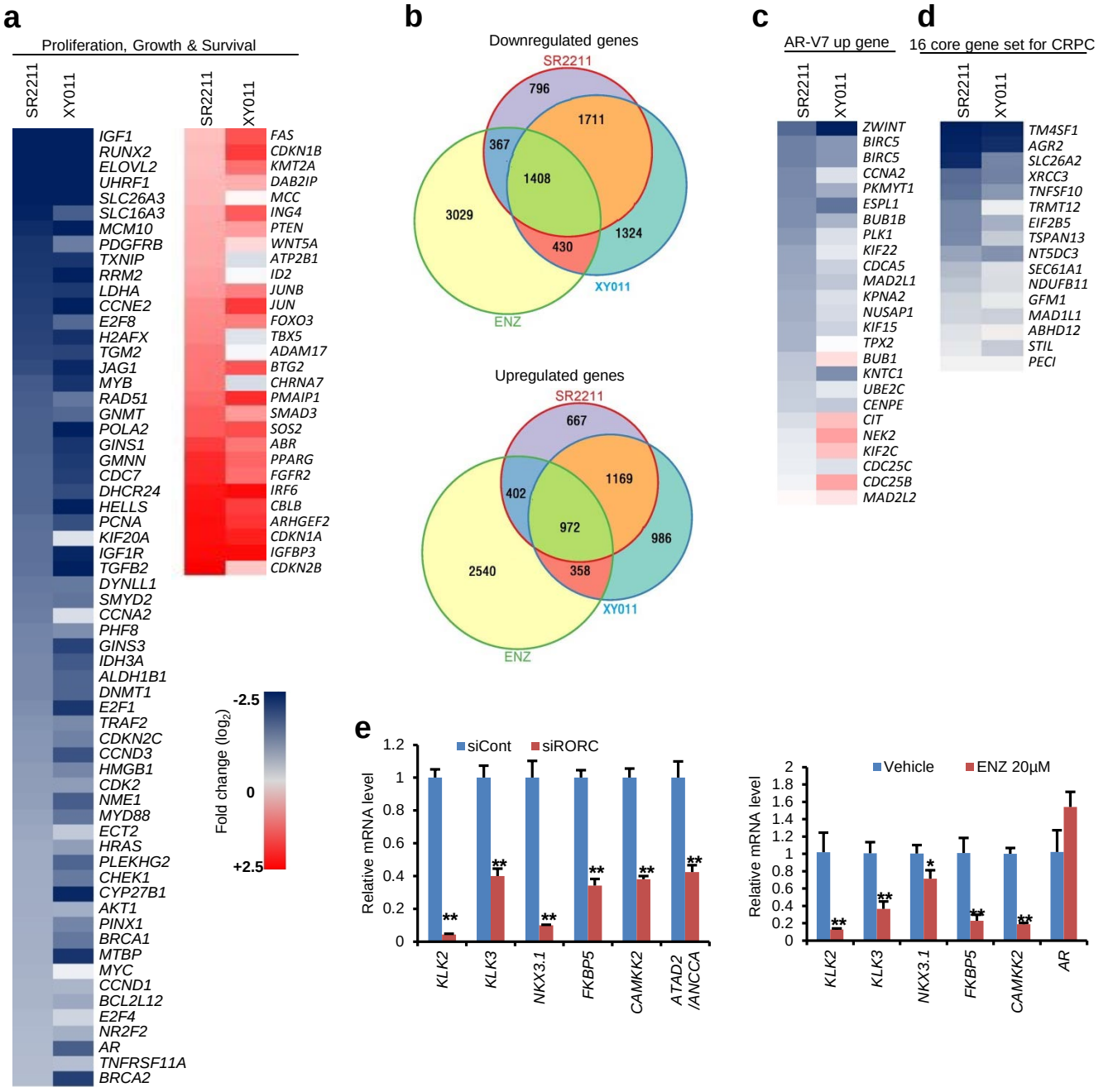

Supplementary Figure 4. ROR-γ antagonists strongly inhibit AR signaling

(a) Heat-map display of the inhibitor-altered expression of genes involved in cell proliferation and survival in C4-2B cells treated with 5 μM SR2211 or XY011 for 48 hours. Gene expression profiling was performed with RNA-sequencing.

(b) Venn diagrams display overlapping number of up- or down-regulated genes (>1.2 fold) in C4-2B cells between SR2211 (5 μM), XY011 (5 μM) and ENZ (20 μM) treatment. Gene expression profiling was performed after RNA-sequencing.

(c) and (d) Heat-map display of the altered expression of AR-V7 up-regulated genes or the core 16-AR CRPC gene set in C4-2B cells treated as above.

(e) qRT–PCR analysis of indicated genes in C4-2B cells treated with indicated siRNA (left) or with ENZ (right) for 48 hours. Data are shown as mean ± s.d. Significance was calculated using Student's *t*-test. ** $p < 0.001$.

Supplementary Figure 5

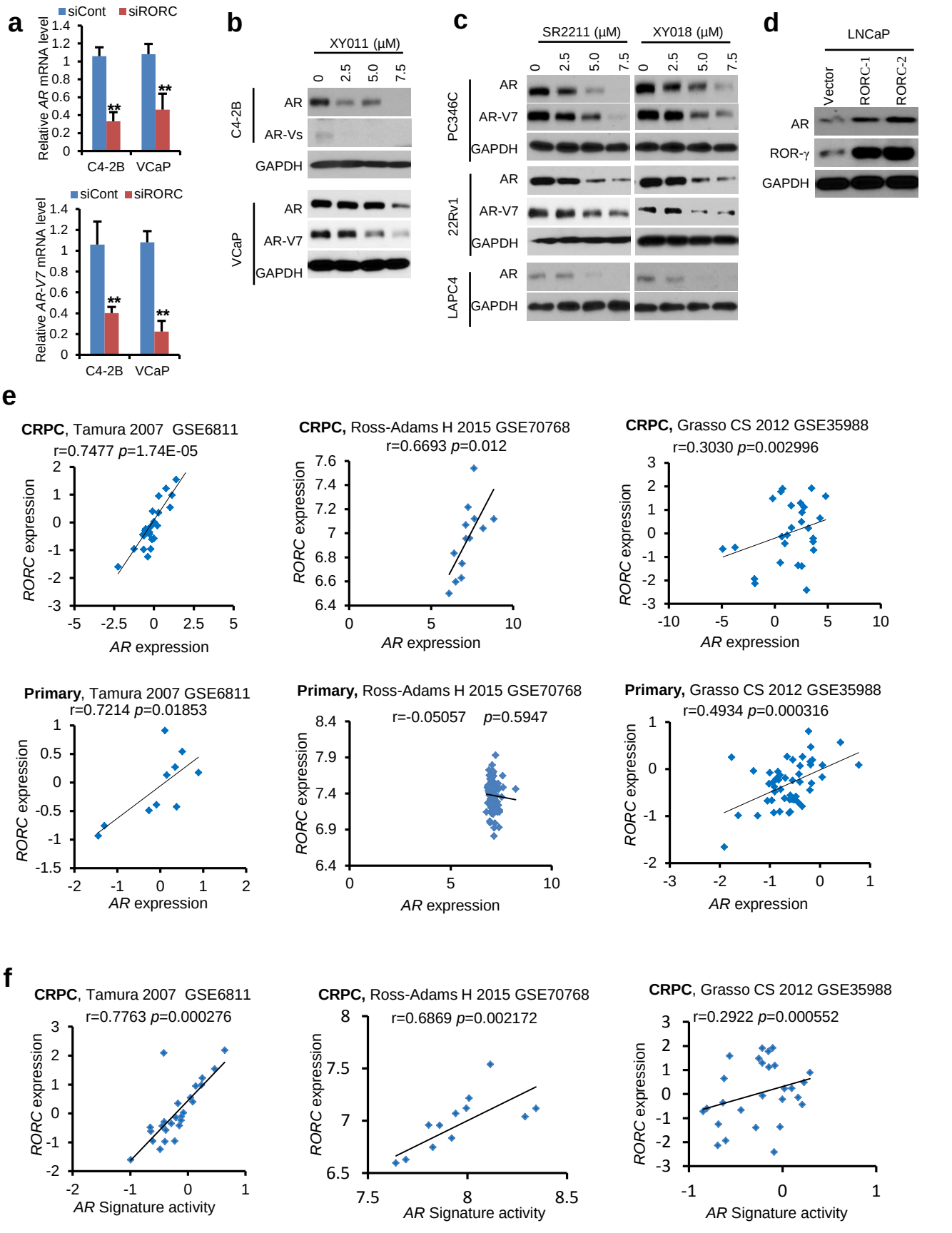

Supplementary Figure 5. Control of AR and its variant expression by ROR-γ in prostate cancer cells and the likelihood in clinical tumors

(a) qRT–PCR analysis of AR full-length and variant AR-V7 expression in C4-2B and VCaP cells treated with indicated siRNAs for 48 hours. Data are shown as mean ± s.d. Significance was calculated using Student's *t*-test. ** $p < 0.001$.

(b) Immunoblotting of AR and its variants or AR-V7 in C4-2B and VCaP cells treated with vehicle or XY011 for 72 hours.

(c) Immunoblotting of AR and its variant AR-V7 in PC346C, 22Rv1 and LAPC4 cells treated with vehicle or XY018 or SR2211 for 72 hours.

(d) Immunoblotting of AR and ROR-γ in LNCaP cells ectopically expressing ROR-γ and the control cells cultured in charcoal-dextran-stripped (cds) FBS supplemented medium.

(e) and (f) Scatter plots showing correlation between ROR-γ and AR gene expression in primary tumors or CRPC tumors. Gene expression profiles are from different clinical data sets (GSE6811, GSE70768 and GSE35988-GPL6480). Scatter plots showing correlation between ROR-γ expression and CRPC AR signature activity in CRPC tumors.

Supplementary Figure 6

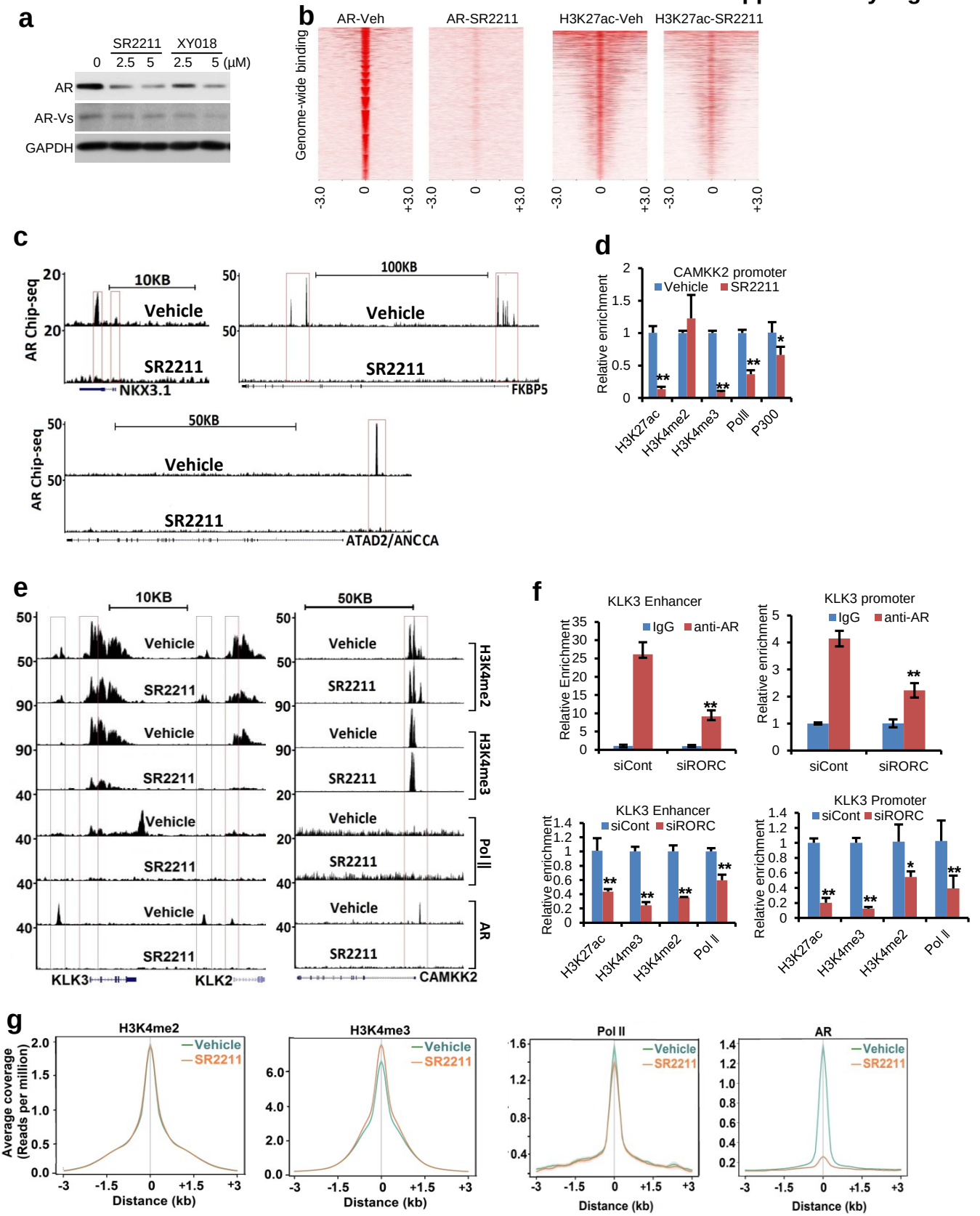

Supplementary Figure 6. The effects of ROR-γ inhibition on AR genome binding, histone modifications, and Pol-II recruitment

(a) Immuoblotting of AR and its variants in C4-2B cells treated with vehicle or SR2211 (5μM) for 24 hours.

(b) A heat-map presentation of AR enrichment (average coverage) across AR-binding sites (ARBS) and H3K27ac enrichment across the enrichment regions in cells treated with vehicle or SR2211 (5μM) for 24 hours in cells treated as in (a).

(c) Genome browser display of AR binding events on the enhancers and/or promoters of AR-target NKX3.1, FKBP5 and ATAD2/ANCCA genes. AR ChIP-seq was performed in C4-2B cells treated for 24 hours with vehicle or SR2211 (5μM).

(d) ChIP-qPCR analysis of relative enrichment of H3K4me2, H3K4me3, H3K27ac, RNA polymerase II (pol II), and acetylase p300 at the promoter of AR-target gene CAMKK2 in C4-2B cells treated with vehicle or SR2211 (5μM) for 24 hours. Data are shown as mean ± s.d. Significance was calculated using Student's *t*-test. ** $p < 0.001$, $n = 3$.

(e) Genome browser display of AR, H3K4me2, H3K4me3 and RNA polymerase II (Pol II) binding events on the enhancers and/or promoters of AR-target KLK2, KLK3 and CAMKK2 genes. ChIP-seq of AR, H3K3K4me2/3 and RNA polymerase II (Pol II) were performed in C4-2B cells treated for 24 hours with vehicle or SR2211 (5μM). Note: the AR ChIP-seq data shown here were obtained from an experiment separate from the data shown in Figure 4.

(f) ChIP-qPCR analysis of relative enrichment of AR, H3K4me2, H3K4me3, H3K27ac, RNA polymerase II (pol II), at KLK3 promoter and enhancer in C4-2B cells treated with control or ROR-γ siRNA for 72 hours. Data are shown as mean ± s.d. Significance was calculated using Student's *t*-test. ** $p < 0.001$, $n = 3$.

(g) Enrichment summary plots of AR, H3K4me2, H3K4me3 and pol II across their corresponding binding sites in different treatment groups. ChIP-seq was performed as in (e).

Supplementary Figure 7

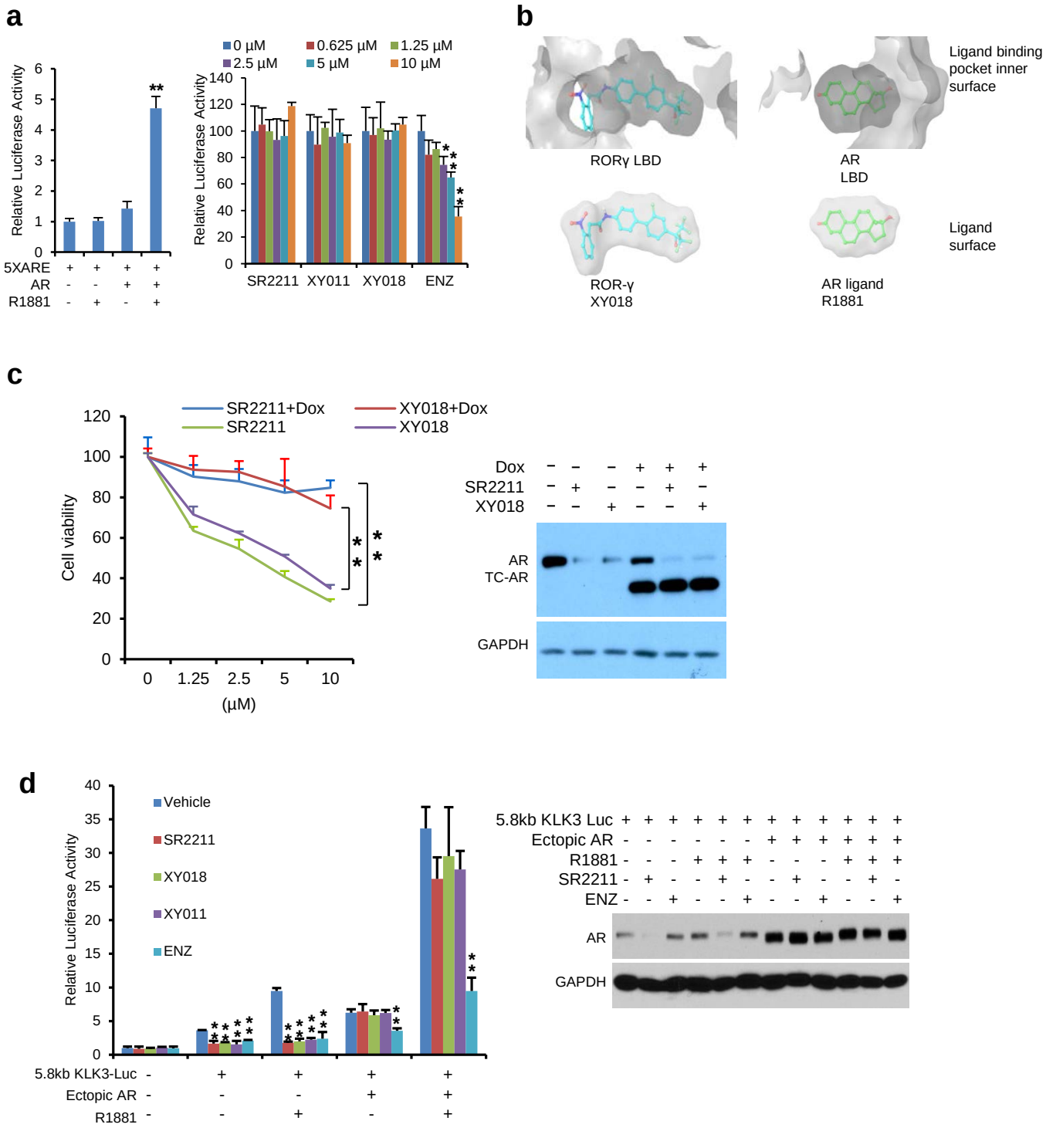

Supplementary Figure 7. ROR-γ antagonists inhibit AR function through suppression of AR expression

(a) Left: 22Rv1 cells in charcoal-stripped medium were transfected with 5×ARE-tk-luc and AR expression construct as indicated. Sixteen hours later, cells were treated with 3 nM R1881 for 24 hours, before harvested for luciferase activity measurement. Right: 22Rv1 cells were transfected as above, and then treated with R1881 and ROR-γ antagonists or AR antagonist (enzalutamide, ENZ) at indicated concentration. * $p < 0.05$, ** $p < 0.01$, $n = 3$.

(b) Molecular docking demonstration that XY018 could snugly dock into the ROR-γ ligand binding pocket but not the AR ligand binding pocket.

(c) LN/TC-AR LNCaP cells were treated with 5 ng/ml doxycycline (Dox) or vehicle for 48 hours before incubating with ROR-γ antagonists (5 μM). After 4 days of antagonist treatment, cells were harvested for cell viability measurements and immunoblotting. ** $p < 0.01$, $n = 3$.

(d) Left: 22Rv1 cells in charcoal-stripped medium were transfected with 5.8kb KLK3-luc and AR expression construct as indicated. Sixteen hours later, and then treated with R1881 (3 nM) and ROR-γ antagonists (5 μM) or AR antagonist (ENZ, 20 μM), before harvested for measuring luciferase activity (left) or immunoblotting with indicated antibodies (right). ** $p < 0.01$, $n = 3$.

Data are shown as mean ± s.d. Significance was calculated using Student's *t*-test.

Supplementary Figure 8

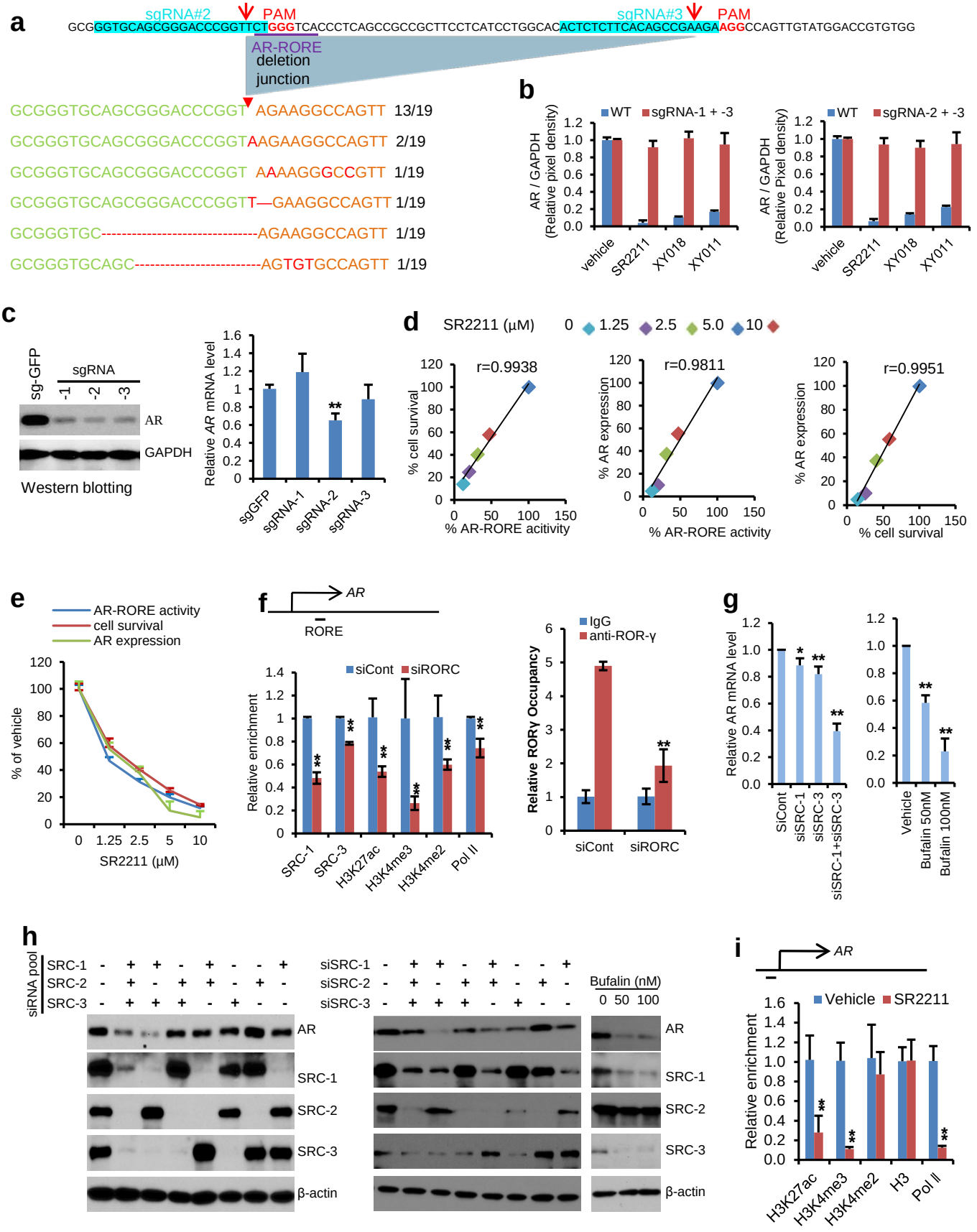

Supplementary Figure 8 ROR-γ directly controls *AR* gene expression through binding to an exonic RORE and recruiting SRCs

(a) Sequencing analysis of the deletion junction of the AR-RORE site. PCR products from sgRNA-2 + sgRNA-3 deleted alleles (Fig. 5c) were cloned and 19 individual clones were sequenced to determine the sequence of deletion junctions and frequency. The top row shows the wild-type sequence and the red arrows indicate expected cleavage sites of Cas9.

(b) Quantitative analysis of RT-PCR products from AR wild type (WT) and indicated sgRNA-deleted alleles in cells treated with vehicle or ROR-γ antagonists. C4-2B cells were infected with lentivirus encoding Cas9 and indicated sgRNAs. After two days, cells were treated with vehicle or the ROR-γ antagonists (5 μM) for another two days before harvested for semi-quantitative RT-PCR. PCR products were separated by agarose gel as shown in Fig. 5e. The experiments were repeated three times. The pixel density of DNA bands from each experiment was quantified as described in ONLINE METHODS and normalized to GAPDH.

(c) Effects of individual sgRNA-mediated alteration of the AR locus on AR expression. Left, immunoblotting of AR and GAPDH with C4-2B cells treated by indicated sgRNA expressing lentivirus. Right, Real-time qRT-PCR analysis of AR expression in C4-2B cells treated as above. ** $p < 0.01$, $n = 3$.

(d) Scatter plot of percentage of indicated inhibitory activities of SR2211 at different concentrations. The results showed a tight correlation between ROR-γ inhibition, AR expression inhibition and anti-proliferation by SR2211. ROR-γ inhibition was measured by reporter gene assay as in Fig. 5f. Anti-proliferation/ cell viability was measured by Cell-Titer GLO as Fig. 2b. AR expression inhibition was analyzed by AR immunoblotting followed by quantification of full-length AR protein bands from three independent experiments as exemplified in Fig. 4a.

(e) Combined plotting of AR-RORE inhibition, AR expression inhibition and anti-proliferation of SR2211 at different concentrations.

(f) ChIP-qPCR analysis of relative enrichment of ROR-γ, H3K4me2, H3K4me3, H3K27ac, RNA polymerase II (pol II) at the AR-RORE site in C4-2B cells treated with control or ROR-γ siRNA for 72 hours. ** $p < 0.01$, $n = 3$.

(g) qRT-PCR analysis of AR expression in C4-2B cells treated with indicated siRNAs (left) or bufalin for 48 hours or 24 hours respectively. * $p < 0.05$, ** $p < 0.01$, $n = 3$.

(h) Left and middle: immunoblotting analysis of indicated proteins in C4-2B cells transfected with smart pool siRNA (left), which were recently used in 2015 Cancer Cell 28, 240-252, by Dr. B.W. O'Malley and his colleagues, or individual siRNA targeting different SRCs (middle) or control siRNAs, individually or in different combinations. Right: immunoblotting analysis of C4-2B cells treated with vehicle or bufalin at indicated concentrations for 2 days.

(i) ChIP-PCR analysis of relative occupancy by H3K4me2, H3K4me3, H3K27ac, Plo II and H3 at AR gene promoter in C4-2B cells treated with vehicle or SR2211 (5 μM) for 24 hours. ** $p < 0.01$, $n = 3$.

Data are shown as mean ± s.d. Significance was calculated using Student's *t*-test.

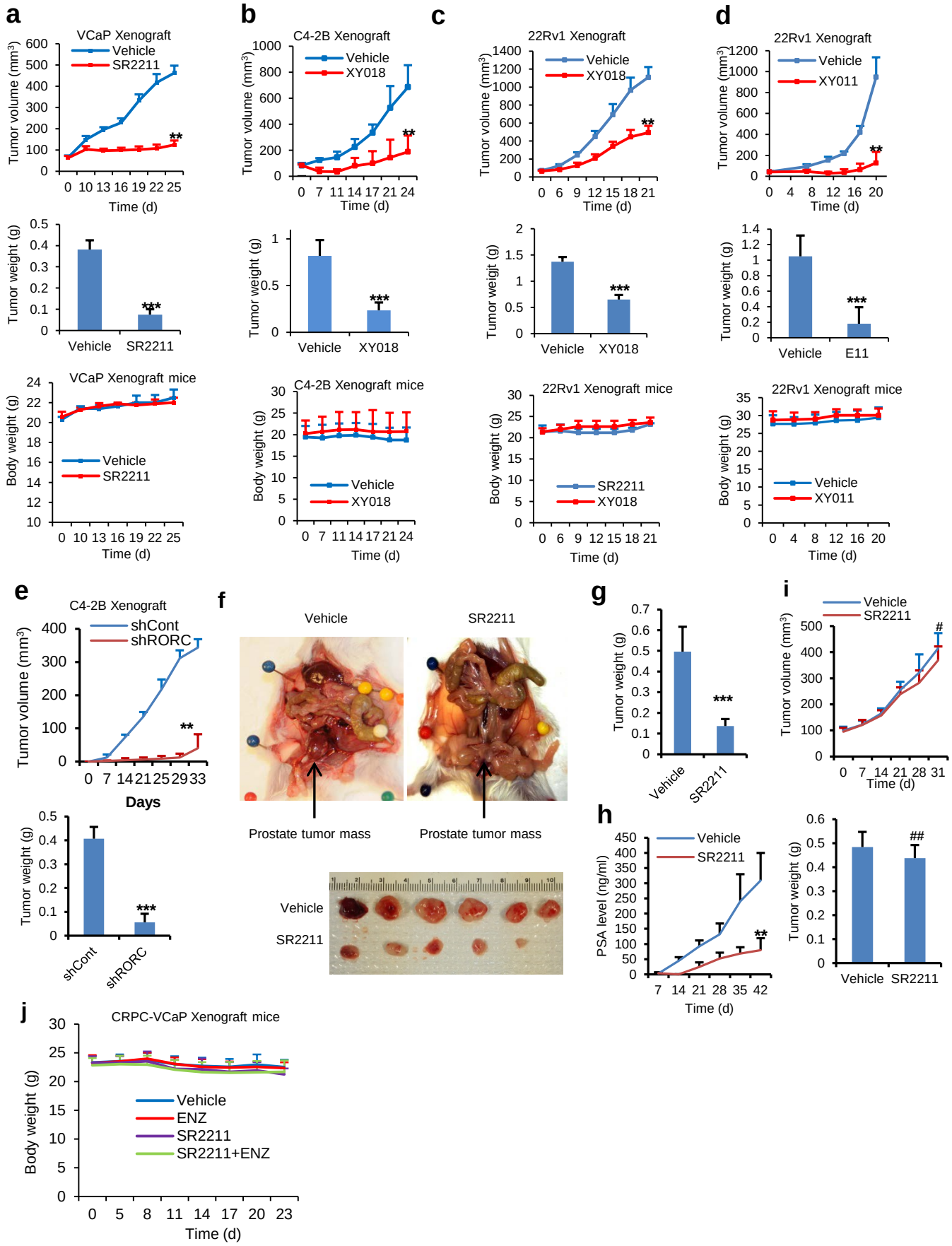
a
VCaP Xenograft
Vehicle
SR2211
Tumor volume (mm3)
Time (d)
Tumor weight (g)
Vehicle
SR2211
VCaP Xenograft mice
Body weight (g)
Time (d)
b
C4-2B Xenograft
Vehicle
XY018
Tumor volume (mm3)
Time (d)
Tumor weight (g)
Vehicle
XY018
C4-2B Xenograft mice
Body weight (g)
Time (d)
c
22Rv1 Xenograft
Vehicle
XY018
Tumor volume (mm3)
Time (d)
Tumor weigit (g)
Vehicle
XY018
22Rv1 Xenograft mice
Body weight (g)
Time (d)
d
22Rv1 Xenograft
Vehicle
XY011
Tumor volume (mm3)
Time (d)
Tumor weight (g)
Vehicle
E11
22Rv1 Xenograft mice
Body weight (g)
Time (d)
e
C4-2B Xenograft
shCont
shRORC
Tumor volume (mm3)
Days
Tumor weight (g)
shCont
shRORC
f
Vehicle
SR2211
Prostate tumor mass
Prostate tumor mass
Vehicle
SR2211
g
Tumor weight (g)
Vehicle
SR2211
i
Vehicle
SR2211
Tumor volume (mm3)
Time (d)
h
Vehicle
SR2211
PSA level (ng/ml)
Time (d)
Tumor weight (g)
Vehicle
SR2211
j
CRPC-VCaP Xenograft mice
Vehicle
ENZ
SR2211
SR2211+ENZ
Body weight (g)
Time (d)

Supplementary Figure 9. *In vivo* effects of ROR-γ antagonists or shRNA on growth of prostate cancer xenograft tumors and mouse body weight

(a) Effects of SR2211 (5 mg/kg, i.p., 5 times a week) or vehicle treatment on growth of VCaP xenografts (n = 8 mice per group). ** p = 2.89E-09, *** p = 3.44E-08.

(b) Effects of XY018 (20 mg/kg, i.p., 5 times a week) or vehicle treatment on growth of C4-2B xenografts (n = 6 mice per group). ** p = 9.92E-06, *** p = 6.69E-05.

(c) Effects of XY018 (5 mg/kg, i.p., 5 times a week) or vehicle treatment on growth of 22Rv1 xenografts (n = 6 mice per group). ** p = 2.7E-04, *** p = 1.55E-05.

(d) Effects of XY011 (20 mg/kg, i.p., 5 times a week) or vehicle treatment on growth of 22Rv1 xenografts (n = 6 mice per group). ** p = 9.99E-08, *** p = 4.71E-06.

(a) to (d): Mean tumor volume ± s.e.m, mean body weight ± s.e.m and mean tumor weight ± s.e.m were shown. Significance was calculated using Student's *t*-test.

(e) Effects of control or ROR-γ shRNA on growth of C4-2B xenografts (n = 6 mice per group). Mean tumor volume ± s.e.m and mean tumor weight ± s.e.m were shown. Student's *t*-test, ** p =3.14E-08, *** p =3.52E-07.

(f) Pictures of orthotopically implanted C4-2B tumors grown in SCID mice treated with vehicle or SR2211 (5 mg/kg, i.p., 5 times a week) for 35 days.

(g) The weights of C4-2B orthotopic tumors from mice treated with SR2211 (5 mg/kg, i.p., 5 times a week) or vehicle (n = 6 mice per group). Mean tumor weight ± s.e.m was shown. Student's *t*-test, *** p = 4.766E-05.

(h) Orthotopic tumor growth was monitored by measuring serum PSA levels on the indicated days. Mean PSA level ± s.e.m was shown. Student's *t*-test, *** p = 1.2683E-05.

(i) Effects of SR2211 (5 mg/kg, i.p., 5 times a week) or vehicle treatment on growth of PC-3 xenografts (n = 6 mice per group). Mean tumor volume ± s.e.m and mean tumor weight ± s.e.m were shown. Student's *t*-test, # p = 0.06, ## p=0.07

(j) Body weight of mice from different treatment groups as in Fig. 6d was shown.

Supplementary Figure. 10

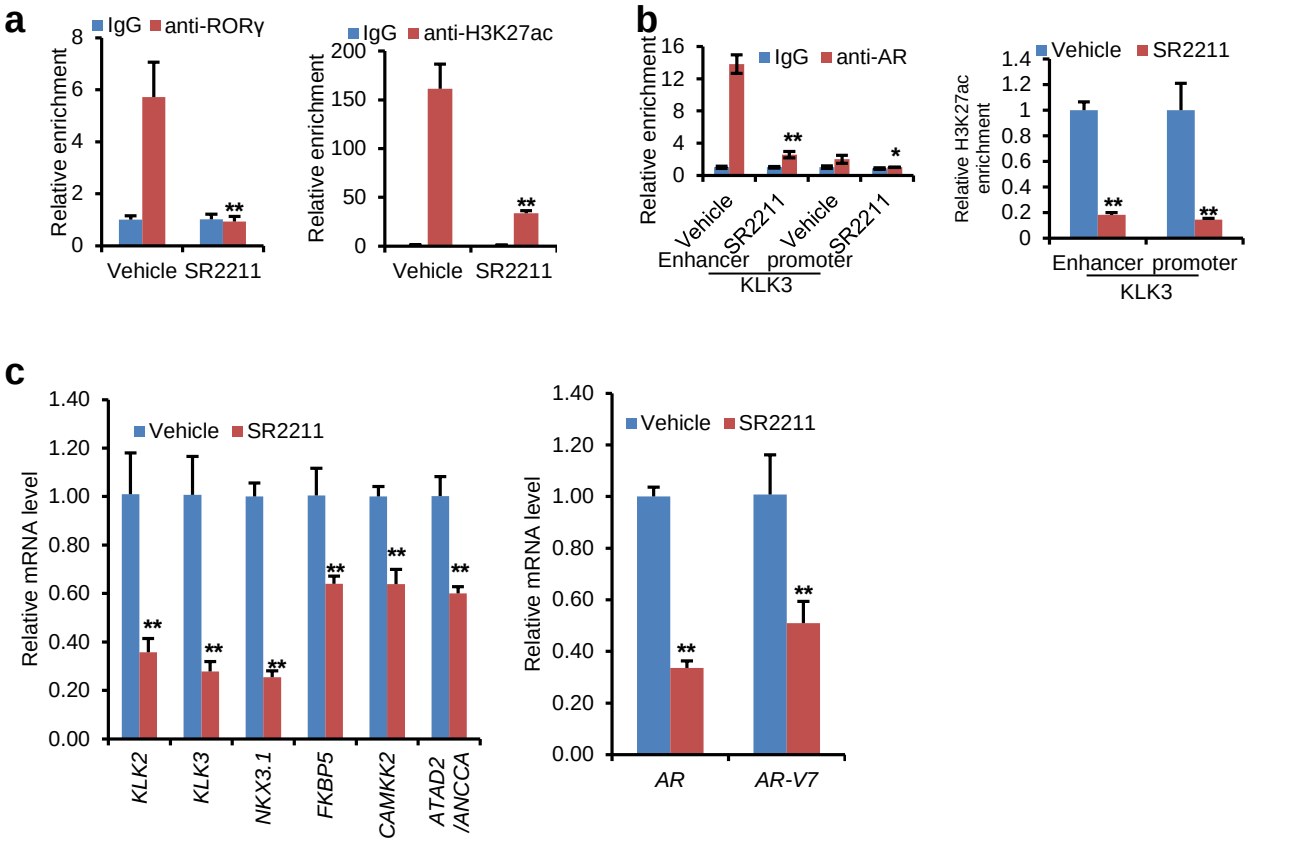

Supplementary Figure 10. ROR-γ inhibition strongly suppresses AR and its variant expression and eliminates AR binding *in vivo*

(a) ChIP analysis of relative ROR-γ occupancy at the AR-RORE site in C4-2B xenograft tumors after treatment with vehicle or SR2211 as in Fig. 6a. Tumors were harvested after 24 days treatment. Three different tumors in each treatment were used for the ChIP assay. ** $p < 0.01$, $n = 3$.

(b) ChIP analysis of relative AR occupancy at the promoter and enhancer ARE sites of KLK3 in C4-2B xenograft tumors after treatment with vehicle or SR2211 as in (a). * $p < 0.05$, ** $p < 0.01$, $n = 3$.

(c) qRT-PCR analysis of AR and AR target gene expression in in C4-2B xenograft tumors after treatment with vehicle or SR2211 as in (a). ** $p < 0.01$, $n = 3$.

Data are shown as mean ± s.d. Significance was calculated using Student's *t*-test.

Supplementary Figure 11

a

Tissue weight (g)	Control	SR2211 (5mg/kg)	*P*-value
Prostate &Seminal Vescle,	0.164 ± 0.006	0.159 ± 0.005	= 0.59
Testis,	0.0983± 0.006	0.0986± 0.004	=0.094
Liver	1.58 ± 0.039	1.61 ± 0.064	= 0.70
Kidney	0.469 ± 0.007	0.458 ± 0.007	= 0.17
Heart	0.135 ± 0.008	0.153 ± 0.007	= 0.15
Spleen	0.109 ± 0.005	0.117 ± 0.008	= 0.47
Lung	0.185 ± 0.008	0.206 ± 0.007	= 0.12
WAT*,	0.129 ± 0.015	0.079 ± 0.005	= 0.01

*WAT : White adipose tissue from epididymal fat pad

b

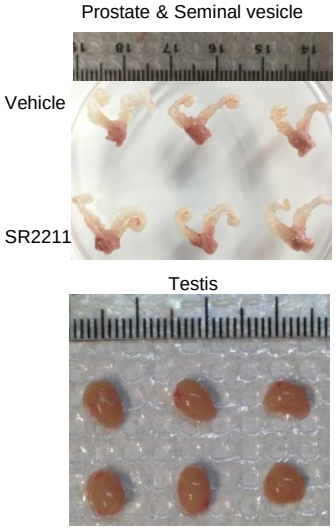

c

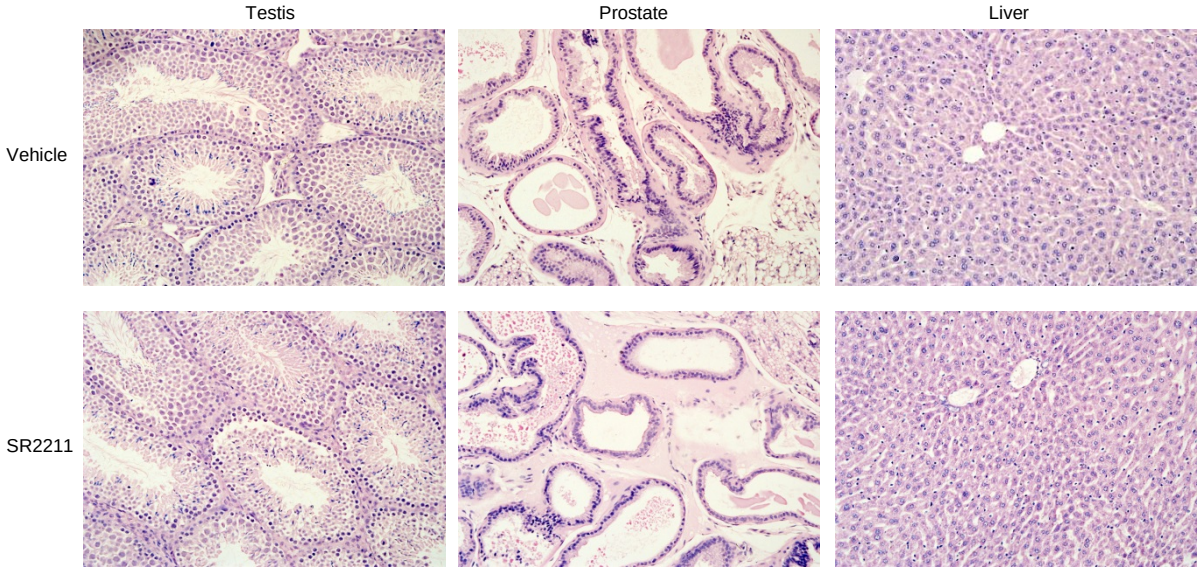

d

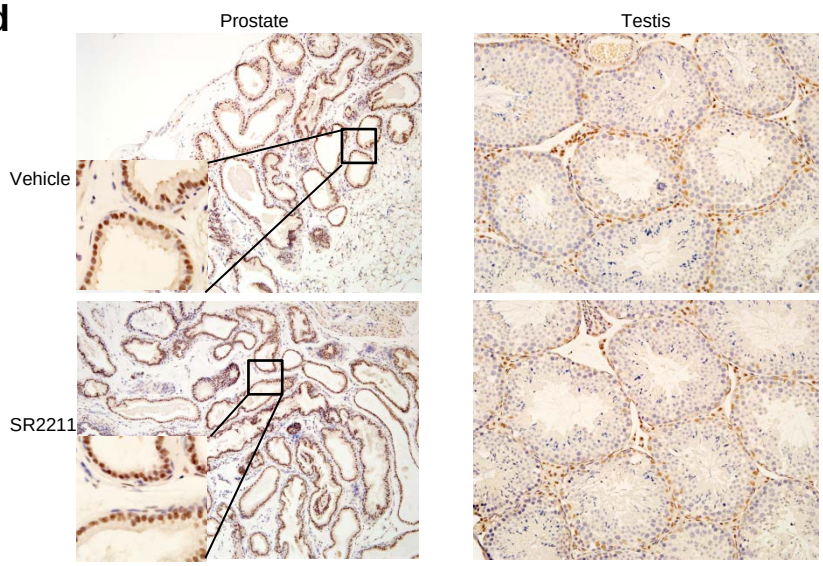

Supplementary Figure 11. *In vivo* effects of ROR-γ antagonists on normal mouse prostate, testis and other tissues

(a) Weight of indicated tissues from mice treated with vehicle or SR2211 for 24 days as in Fig. 6a of C4-2B xenograft model. Significance was calculated using Student's *t*-test, * $p = 0.01$, $n = 6$.

(b) Representative images of seminal vesicle and prostate, and testis from mice treated with vehicle or SR2211for 24 days were shown.

(c) Representative H&E images of prostate, testis and liver from vehicle- or SR2211-treated mice.

(d) Representative anti-AR IHC images of prostate and testis sections from mice treated with vehicle or SR2211.

Supplementary Figure 12

a

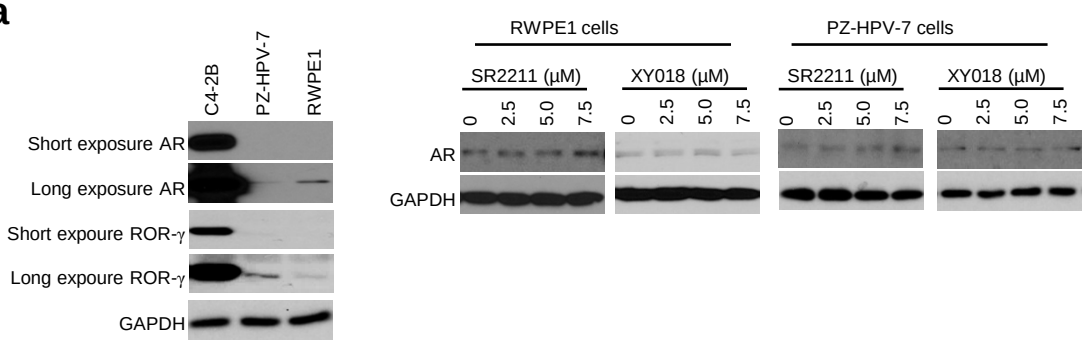

b

Supplementary Figure 12. Lack of inhibitory effects by ROR-γ antagonists on AR expression in non-malignant, human prostate epithelial cells

(a) Immunoblotting analysis of ROR-γ and AR expression in in non-malignant, human prostate epithelial RWPE1 and PZ-HPV7 cells with indicated treatments.

(b) Comparison of genomic DNA sequences at the 3' end region of AR exon1 between different species with sequences matching the RORE motif highlighted in red and deviations in green. Note: the corresponding murine sequences (CTGGATCG) are predicted to be nonfunctional as a RORE because of the two nucleotide deviations from consensus RORE motif as reported in previous studies.

Supplementary table 1 antibodies for immunoblotting

Antibody	Vendor	Catalogue number	dilution
ACTR	Upstate	05-490	1:1000
ERG	Epitomics	2805-1	1:1000
AR	NeoMarkers	MS-443-P0	1:1000
AR-V7	Precision antibody	AG10008	1:1000
BCL-XL	Santa Cruz	sc-8392	1:500
CDC2	Santa Cruz	sc-54	1:500
CDC6	Santa Cruz	sc-9964	1:500
CDK4	Santa Cruz	sc-260	1:500
cleaved-Caspase7	Cell signaling	#9491	1:1000
cleaved-PARP1	Cell signaling	#9542	1:1000
CyclinA2	Cell signaling	#4656	1:1000
CyclinD1	NeoMarkers	RB-9041-P1	1:1000
CyclinD3	Santa Cruz	sc-182	1:500
CyclinE2	Santa Cruz	sc-9566	1:500
GAPDH	Cell signaling	#2118	1:4000
Myc	Santa Cruz	sc-764	1:500
PSA	NeoMarkers	MS-260-P1	1:1000
RORγ	Ebioscience	14-6988-82	1:500
SRC-1	Santa Cruz	sc-8995	1:1000
β-actin	Santa Cruz	sc-47778	1:2000
TIF2	BD	610985	1:500

Supplemental table 2 Primers for qPCR and ChIP assay

Primers for qPCR		
CAMKK2 qrt-F	TGAAGACCAGGCCCGTTTCTACTT	
CAMKK2 qrt-R	TGGAAGGTTTGATGTCACGGTGGA	
ATAD2/ANCCA qRT-F	CACCGAGTACTCCTGTGGCTTG	
ATAD2/ANCCA qRT-R	TCTAGCTCGAGTCATTCGCAGAACAC	
FKBP5 qRT-F1	GGG AAG ATA GTG TCC TGG TTA G	
FKBP5 qRT-R1	GCA GTC TTG CAG CCT TAT TC	
NKX3.1 qRT-F	CCA TAC CTG TAC TGC GTG GG	
NKX3.1 qRT-R	TGC ACT GGG GGA ATG ACT TA	
KLK3/PSA qRT-F1	GGA AAT GAC CAG GCC AAG AC	
KLK3/PSA qRT-R1	CCA GCT TCT GCT CAG TGC TT	
KLK2 qRT-F2	CAACATCTGGAGGGGAAAGGG	
KLK2 qRT-R2	AGGCCAAGTGATGCCAGAAC	
AR-FL-qRT-F	ACATCAAGGAACTCGATCGTATCATTGC	
AR-FL-qRT-R	TTG GGC ACT TGC ACA GAG AT	
AR-V7-qRT-F	CCATCTTGTCGTCTTCGGAAATGTTATGAAGC	
AR-V7-qRT-R	TTT GAA TGA GGC AAG TCA GCC TTT CT	
β-Actin F	GAGAAAATCTGGCACCACACC	
β-Actin R	ATACCCCTCGTAGATGGGCAC	

Primers for ChIP assay		
PSA promoter-F1	GCC AAG ACA TCT ATT TCA GGA GC	
PSA promoter-R1	CCC ACA CCC AGA GCT GTG GAA GG	
PSA promoter-F2	TCC TGA GTG CTG GTG TCT TAG	
PSA promoter-R2	AGC CCT ATA AAA CCT TCA TTC CCC	
PSA enhancer-F1	TGGGACAACTTGGAAACCTG	
PSA enhancer-R1	CCAGAGTAGGTCTGTTTTCAA	
PSA enhancer-F2	AGGACAGTCTCAACGTTCCACCAT	
PSA enhancer-R2	TGCCTTATTCTGGGTTTGGCAGTG	
CAMKK2 promoter F1	AGAACACTGTAGCTCACACAGGCA	
CAMKK2 promoter R1	GGGCACTTCCCAACCTTTCTTACT	
CAMKK2 promoter F2	AAAATGTGAAAGGCCAGGTG	
CAMKK2 promoter R2	AAAGCAGGGTTGCCAAACTA	
AR chip -5.1KB F	GGTTTGAAACCTCTGATGCAGG	
AR chip -5.1KB R	CTGTCCTCAATGTTGAAGCCATC	
AR chip -3.2KB F	GTG TAT ACC TAC CCT GTG ACT C	
AR chip -3.2KB R	CTG TAC CAC GCT TTG TTT ATC C	
AR chip -2.5KB F	GGC AGA TGT GTG AGA TAC TTA G	
AR chip -2.5KB R	CAG AGG TGT TCT CTC AGA TTA G	
AR chip -1.7KB F	GTG TAG ACA CAT AGT TCT CCT G	
AR chip -1.7KB R	CCT TCC TTG AAT ATA CCT CAC C	
AR chip -1KB F	CCC AGA ATC AGA AGT CAA AGG A	
AR chip -1KB R	GTC CCA TAA GCC CTG TGT AAA G	

AR chip -0.4KB F	GCA GGT ATT CCT ATC GTC CTT T	
AR chip -0.4KB R	CTG AAT AGC TCC TGC TTT CCT A	
AR chip +0.9KB F	CTT CTT CTG CAC GAG ACT TTG A	
AR chip +0.9KB R	TCT TCC ACC TAC TTC CCT TAC C	
AR chip +1.7KB F	CCT GTT GAA CTC TTC TGA GCA	
AR chip +1.7KB R	CTG GAA CAG ATT CTG GAA AGC	
AR chip +2KB F	TTC AAG GGA GGT TAC ACC AAA G	
AR chip +2KB R	CAG AGC CAG TGG AAA GTT GTA G	
AR chip +2.3KB F	TAC CCT GTC TCT CTA CAA GTC C	AR-RORE
AR chip +2.3KB R	TAG TCC AGC GGG TTC TCC AG	AR-RORE
AR chip +2.8KB F	GAG GGT GGA GTG AGG TTT TT	
AR chip +2.8KB R	CAA CTG CGG TGA GGA ATA AT	
AR chip +3KB F	ATT CCT CAC CGC AGT TG	
AR chip +3KB R	ATT TCG GAG AAG TCA CAG GT	
AR chip +24KB F	AAA CGA ATG CAG AGT GCT CCT	
AR chip +24KB R	GTC ACA GTC CAA ACC TTA CAA	
AR chip +96KB F	ATA GCA GCC ATA TCA GAT GGG	
AR chip +96KB R	TGT GAT TGA GCA TTT CCC CTG	
AR chip +98KB F1	GGT GAC TAA TCC CAG ATC CTA	
AR chip +98KB R1	TTA CCC AGC AAT GAT CAC AAG	
AR chip +98KB F2	CTT GTG ATC ATT GCT GGG TA	
AR chip +98KB R2	TGA TCT GTA CCA AAC AGC AC	
AR chip +115KB F	AGA TCA CTC TCG ACT AGC AAG	
AR chip +115KB R	GGC TTA TCT GCA GGA TCC ATT	
AR chip +170KB F	CCA GTT GAG TGC AAC TAA TCC	
AR chip +170KB R	GCG GCA CAT AGA AGT TCA GTA	
AR chip +190KB F	GCC TTT GGA GTC ATA GCT AAG	
AR chip +190KB R	GAC AAC TTG ATA TCC ACG TGC	
AR chip +225KB F	AGA TCA AGG GAA GCA ACA GTC	
AR chip +225KB R	TTA TGC AGC CTG CAG AAC CAT	

Supplemental table 3 siRNA sequence

Gene	Sequence	Vendor and Cat. No
siRORC-1	CGAGGATGAGATTGCCCTCTA	Dharmacon
siRORC-2	CACCTCACAAATTGAAGTGAT	Dharmacon
siCont	CAGTCGCGTTTGCGACTGG	Dharmacon
SRC-1	CUAGCUGAGUUACUGUCUGCC	Dharmacon
SRC-2	CGAAGAGCAAACUCAUCCGUU	Dharmacon
SRC-3	GAUUACUGCAGAAGCCACUGG	Dharmacon
SRC-1 smart pool siRNA	A-005196-17 GUAUUAGCUCACAAUUAGA A-005196-18 GGUGGAAAUACGAAUGUUC A-005196-17 CUAGCAGAUUAAAUAUACA A-005196-17 GGGUGGAUUAGAUGUAUUA	Dharmacon, E-005196-00-0005
SRC-2 smart pool siRNA	A-020159-13 GGACAAGGGUUGAAUAUGA A-020159-14 UAAUGAACCUCAACUUGUA A-020159-15 GCAAUAAUUUAAGUUGAGA A-020159-16 UUGCUAAGUAUUGAAUUUC	Dharmacon, E-020159-00-0005
SRC-3 smart pool siRNA	A-003759-18 CUCUGGGCUUUUAUUGCGA A-003759-18 CUGAUAUCUGCCAAUCUUA A-003759-18 GCAGCAGUAAUGAUGGAUC A-003759-18 CUACCAAGUUCAAAAUAUA	Dharmacon, E-003759-00-0005